Polymer Journal, Vol. 28, No. 11, pp 992—999 (1996)

Solid-State Structure of Comb-Like Polymers Having *n*-Octadecyl Side Chains II. Crystalline-Amorphous Layered Structure

Katsuhiro INOMATA, Yoshiaki SAKAMAKI, Takuhei NOSE, and Shintaro SASAKI*

Department of Polymer Chemistry, Tokyo Institute of Technology, 2–12–1 Ookayama, Meguro-ku, Tokyo 152, Japan
**Department of Chemical Materials Science, School of Materials Science, Japan Advanced Institute of Science and Technology, Asahidai, Tatsunokuchi, Ishikawa 923–12, Japan*

(Received June 6, 1996)

ABSTRACT: Crystalline-amorphous layered structure constructed by comb-like poly[(methyl acrylate)-*stat*-(*n*-octadecyl acrylate)]s (PA*x*), which have crystallizable *n*-alkyl side chains and amorphous main chain, has been investigated by X-ray diffraction method. Small-angle X-ray scattering profiles of PA*x* and its blends with *n*-octadecanoic acid (C18) varies with the change of $1/f_{main}$, which is defined as the ratio of the number of the *n*-alkyl side chain and C18 molecule to that of the main chain $-CH_2-CH-$ unit. When $1/f_{main}$ is smaller than 0.71, the layer spacing obtained from diffraction angle of a sharp peak at small-angle region gradually decreases with an increase of $1/f_{main}$. In the region of $1/f_{main}=0.73$—0.89, a broad peak coexists with the sharp peak, and locates at smaller angle region than the sharp peak. When $1/f_{main}$ is larger than 1.0, *i.e.*, blends of poly(*n*-octadecyl acrylate) (PA100) with C18, a newly appeared sharp reflection can be observed at further smaller angle. These complicated variations in layer spacing are interpreted by three packing models, which are named as Interdigitating Form, End-to-end Form, and disordered End-to-end Form, respectively. Differential scanning calorimetry measurements for PA100/C18 blends also suggest the existence of another crystalline form induced by the addition of C18. In the blends of PA100 with *n*-tetradecanoic acid, the chain length of which is shorter than C18, the structural transformation observed in PA100/C18 system can not be recognized.

KEY WORDS Comb-Like Polymer / *n*-Alkyl Fatty Acid / Poly(*n*-octadecyl acrylate) / Layered Structure / X-Ray Diffraction / Layer Spacing / Packing Manner /

Comb-like polymers, in which crystallizable long *n*-alkyl side chains attach to amorphous main chain, have been extensively studied as reviewed by Platé and Shibaev.[1] In these polymers, the side chains are known to crystallize in solid state irrespective of their tacticity of main chain. X-Ray diffraction and differential scanning calorimetry (DSC) measurements suggest the formation of hexagonally-packed crystalline lattice of *n*-alkyl chain. In the X-ray profile at small-angle region, there exists an intense reflection, which is considered to originate from alternating crystalline-amorphous layered structure constructed by the side-chain-crystallized layer and main-chain-segregated amorphous layer as shown in Figure 1. The domain spacing of the layered structure, *d*, can be obtained by the diffraction angle of this reflection. Platé *et al.*[1,2] reported striking difference in the diffraction pattern and layer spacing *d* between comb-like polyacrylates and polymethacrylates. In the diffractogram of poly(*n*-octadecyl acrylate), a relatively broad reflection was observed at small-angle region and its spacing was larger than 40 Å, and in that of poly(*n*-octadecyl methacrylate), a sharp reflection was observed at the spacing of *ca.* 30 Å. In order to interpret this difference in X-ray profiles, they proposed two chain-packing models: two-layer structure and one-layer structure for respective polymers.[1,2] In the former model, the side chains extend on both side of the main chain, and the polymer chains pack closely because of the flexibility of the main chain. In the latter structure, disordered packing of the end groups of the side chains occurs because of the increased bulkiness of the main chain, and the polymer chains are arranged with the shift toward the extended side-chain axis, which leads

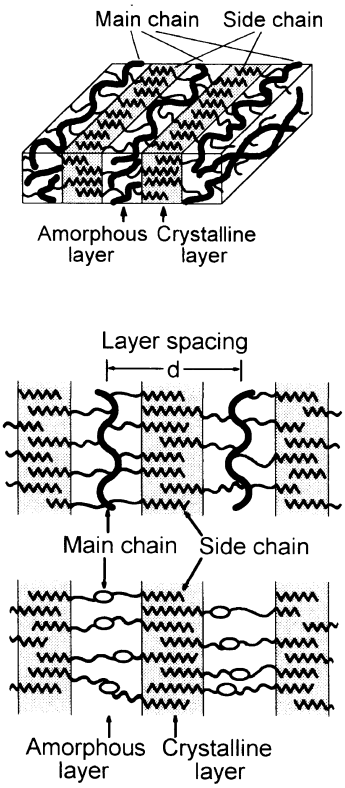

Figure 1. Schematic illustration of the alternating crystalline-amorphous layered structure constructed by side-chain-crystallizable comb-like polymer. The middle and bottom figures is the projection of the upper figure viewed as perpendicular to the main chain and viewed along the main chain, respectively. Thick lines in the middle figure and ellipses in the bottom figure represent the main chain, thin lines represent the side chain, and notched thin lines represent the crystallized side chain. The hatched domain is the crystalline layer. The layer spacing *d* is also indicated.

the layer spacing to be smaller value. Later, Hsieh *et al.*[3] proposed a new model for solid-state poly(*n*-octadecyl methacrylate). In their model, the crystalline layer is formed by intercalating the side chains pointing in opposite directions. They have mentioned that this model can explain the experimentally-obtained intensity distribution of X-ray reflections in small-angle region. Although detailed solid-state structures of these comb-like polymers have not been clarified as yet, the layered structure with the alternating segregation of the side-chain and main-chain domains is commonly accepted.[4-8]

The layered structure in Figure 1 recalls a lamellar morphology observed in, for example, A–B diblock copolymers. Microphase separation of block or graft copolymers having incompatible block segments has been widely interested and investigated by a large number of researchers.[9-14] Equilibrium aspects of the microdomain structure involve two requirements, *i.e.*, incompressibility and incompatibility. When A and B blocks in A–B diblock copolymer are strongly incompatible, each segment segregate into the confined A and B domains, respectively. The incompressibility demands uniform overall segment density everywhere in the domain space. Morphology of the domain structure depends on the molecular weights of the constituent block segments and the interaction parameter between A-block and B-block segments.

In Part I of this series,[15] we have reported cocrystallization behavior of blended *n*-octadecanoic acid (C18) with *n*-octadecyl side chains of poly[(methyl acrylate)-*stat*-(*n*-octadecyl acrylate)] (PA*x*) and poly-[(methyl methacrylate)-*stat*-(*n*-octadecyl methacrylate)] (PM*x*), where *x* is the composition of *n*-octadecyl ester residue in mol%. In the cocrystallized solid, C18 molecules are incorporated into the hexagonal crystalline lattice formed by the side chains.[15] The cocrystallization of C18 with the side chain in the crystalline layer will increase the volume of this layer, and is anticipated to influence the segregation behavior and packing manner of the chains in the layered structure.

In this report, we aim to investigate the layered structure of the comb-like PA*x* series, and their blends with *n*-alkyl fatty acid, Cn, where n is the number of carbon atoms in the fatty acid. Small-angle X-ray scattering profiles of these polymers vary complicatedly with the change of the composition of the *n*-octadecyl side chain in pure PA*x* or the content of Cn in the blend samples. These changes are reasonably interpreted by three kinds of packing model with considering volume of the crystalline and amorphous layers and area of the interface between them. The effect of chain length of blended fatty acid on the layered structure will also be discussed.

EXPERIMENTAL

Poly[(methyl acrylate)-*stat*-(*n*-octadecyl acrylate)]s (PA*x*) were prepared as described in the previous paper.[15] In this work we use six kinds of copolymer, PA33, PA54, PA70, PA81, PA89, and PA100, the number in these codes represents the composition of the *n*-octadecyl ester residue in copolymer in mol%. *n*-Tetradecanoic acid (C14), *n*-hexadecanoic acid (C16), *n*-octadecanoic acid (C18), *n*-eicosanoic acid (C20), and *n*-docosanoic acid (C22) were commercially available and used without further purification. Blend samples of PA*x* with Cn were prepared by evaporation of solvent from tetrahydrofuran solution, annealing at 90°C, and subsequently cooled slowly to room temperature.

X-Ray diffraction measurements were performed with Ni-filtered Cu-K_α radiation (wave length $\lambda = 1.5418$ Å) generated from RU-200BH (Rigaku Co.) and an imaging plate detector (R-AXIS IID, Rigaku Co.) at room temperature. The distance between the sample and the imaging plate was calibrated by the 111 reflection of silicon powder sprinkled over the sample. Diffraction diagrams recorded on the flat imaging plate were converted to the one-dimensional profiles against diffraction angle 2θ. DSC thermograms were recorded by a Perkin-Elmer DSC model II instrument.

RESULTS

Variation of X-ray diffraction profiles for pure PA*x*'s with the change of the composition of *n*-octadecyl side chain, *x*, is shown in Figure 2. Diffraction angle 2θ of a sharp peak increases with an increase of *x* for PA33, PA54, and PA70. In the case of PA81, a broad peak is also observed at an angle smaller than that for the sharp peak. Both these two peaks can be recognized in the profile of PA81 and PA89, and in that of PA100, only the broad peak can be observed. As mentioned in Introduction, these reflection peaks are considered to originate from the alternating crystalline-amorphous layered structure. So, the variation of the X-ray profiles suggests a change of the packing manner of chains and a change of the arrangement of the crystalline and amorphous layers.

The profiles of PA70, PA81, and PA89 in Figure 2 are comparable with those of the blend samples PA70/C18 presented in Figure 6 in Part I of this series.[15] In Part I, we have reported that the addition of C18 to PA70 induces the formation of the layered structure observed in PA100. From the resemblance between the profiles of pure copolymers (Figure 2) and blends of PA70/C18 (Figure 6 in Part I[15]), we can say that the added C18

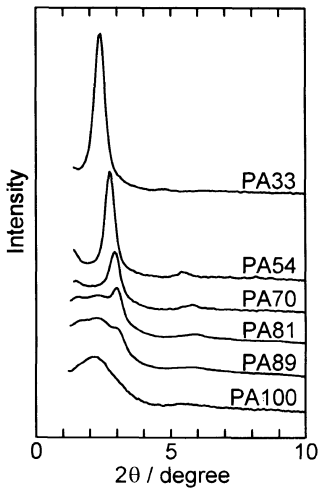

Figure 2. X-Ray diffraction profiles for pure copolymer PA*x*'s, as shown, measured at room temperature. The base line for each profile is shifted up and down in order to avoid overlapping.

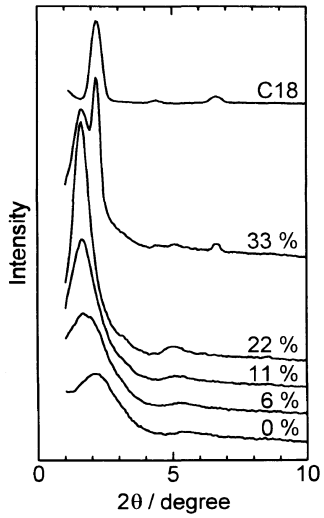

Figure 3. X-Ray diffraction profiles for PA100/C18 blends with the shown C18 contents (mol%). All measurements are performed at room temperature. The base line for each profile is shifted up and down in order to avoid overlapping.

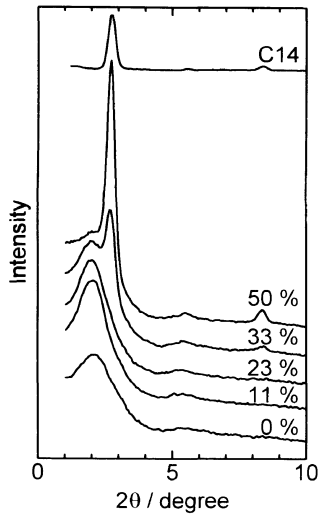

Figure 4. X-Ray diffraction profiles for PA100/C14 blends with the shown C14 content (mol%). All measurements are performed at room temperature. The base line for each profile is shifted up and down in order to avoid overlapping.

molecules behave as the *n*-alkyl side chain for the formation of the layered structure.

Distinct change in profile is observed in the system of PA100/C18. As shown in Figure 3, the blend with 6 mol% C18 gives a sharp peak at an angle smaller than that of pure PA100, and further addition of C18 increases the scattering intensity of this peak. The profiles of pure PA100 and C18 show peaks at $2\theta = 2.1°$ and 2.2°, respectively, while the peak of the blend is located at $2\theta = 1.6°$. As confirmed by the absence of the diffraction peaks assignable to the isolated C18 crystallite, C18 molecules are cocrystallizing homogeneously with *n*-octadecyl side chain till the C18 content of 22 mol%. These considerable changes in the shape and the scattering angle of the peak should mean the formation of another arrangement of the layered structure by the addition of C18.

The shift to the smaller-angle region and increase of the intensity for the peak in the X-ray profile are also recognized in the blends of PA100 with C20 or C22. However, as shown in Figure 4, PA100/C14 blends do not show such sudden change in the profile until the crystallization of the isolated C14 occurs.

DISCUSSION

Variation of X-Ray Profiles of PAx/C18 with the Change of $1/f_{main}$

The similarity between the X-ray profiles in Figure 2 and those in Figure 6 in Part I suggests that C18 molecules cocrystallize with the side chain of polymer[15] and behave such as the side chain for the formation of the layered structure. With taking this behavior into consideration, we can say that the X-ray scattering profile in the small-angle region for PA*x*/C18 system is determined by the number of *n*-alkyl chain in the sample. In Part I, we have defined the ratio of the number of the repeating unit of the main chain to that of the *n*-alkyl chain as f_{main}, in order to compare the results of DSC measurements of pure polymers with those of their blends with C18.[15] In the number of the *n*-alkyl chain, both *n*-octadecyl side chain and C18 molecule are included. Reciprocal of f_{main} corresponds to the composition of *n*-octadecyl side chain of the pure copolymer, *i.e.*, $1/f_{main} = x/100$. We will use the parameter $1/f_{main}$ in order to represent the relative amount of crystallizable *n*-alkyl chain (both *n*-octadecyl side chain and C18 molecule) to the repeating unit of the amorphous main chain (–CH_2–CH– group).

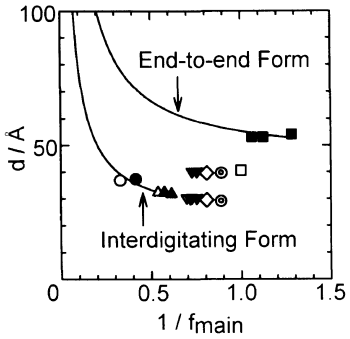

Figure 5. Observed and calculated layer spacings *d* for PA*x*/C18 against $1/f_{main}$, which is defined as the ratio of the number of *n*-alkyl chain to that of repeating unit of main chain. The experimental values of *d* for pure copolymers, PA*x*, and blend samples, PA*x*/C18, are plotted by open and filled symbols, respectively, with the same shape: (○, ●) PA33; (△, ▲) PA54; (▽, ▼) PA70; (◇) PA81; (◎) PA89; (□, ■) PA100. The solid lines are calculated with assuming Interdigitating Form and End-to-end Form as shown in the figure.

In Figure 5, the layer spacings $d = \lambda/(2\sin\theta)$ obtained for six kinds of pure PA*x*'s are plotted against $1/f_{main}$ by the open symbols, and the results for their blends with C18 are plotted by the filled symbols which are the same shape as those of the respective pure PA*x*. The data in this figure are the only results for the blend samples in which no crystallite of isolated C18 is confirmed. For the pure copolymers PA33, PA54 and PA70 ($1/f_{main} = 0.33$, 0.54, and 0.70), and their blends with C18, the obtained *d* values smoothly decrease with the increase of $1/f_{main}$. This result indicates that the addition and cocrystallization of C18 give a similar effect on the formation of the layered structure with the increase of *n*-octadecyl side-chain composition. We can summarize the variation of

the X-ray profiles as follows: (1) in the range of $1/f_{main}=0.33$—0.70, the layer spacing obtained from the sharp peak gradually decreases with the increase of $1/f_{main}$, (2) when $1/f_{main}=0.73$—0.89, both the broad and sharp peaks can be observed, and only the former peak is observed when $1/f_{main}=1.0$: *i.e.*, in the case of the pure PA100, and (3) the sharp peak of $d>50$ Å appears in the range of $1/f_{main}=1.06$—1.28: *i.e.*, in the case of the blends PA100/C18.

Analyses of the Layered Structure

The discontinuity of the value of d with the increase of $1/f_{main}$ in Figure 5 suggests a transformation of the layered structure, *i.e.*, change of the packing manner of chains and rearrangement of the crystalline and amorphous layers. Although some structural models for these comb-like polymers have been proposed[1-4] as described in Introduction, it seems to be difficult to interpret these experimental results shown in Figure 5 by these models. Main factor that determines the packing manner of the comb-like polymers in solid state may be segregation of the crystallizable *n*-alkyl side chains and amorphous main chains. Because of the covalent bonds between the side chain and main chain, the segregation will result in the alternating crystalline and amorphous layers. Schematic molecular structure in solid state is shown in Figure 6. If the crystallizable and amorphous segments are segregated distinctly and the interface between the crystalline and amorphous layers is sharp (see Figure 6), the domain spacing of the amorphous layer can be determined from its volume and the area of the interface owing to the demand of incompressibility of the segments.[12-14] We assume that the tacticity of the comb-like polymer is atactic, and that the distribution of the position of the long side chains along the main chain is statistically random. On these assumptions, we propose two structural models for the packing of the comb-like polymers in the alternating crystalline and amorphous layers. These are schematically illustrated in Figures 7a and 7b, and named as Interdigitating Form and End-to-end Form, respectively. Interdigitating Form corresponds to the structural model proposed by Hsieh *et al.*,[3] and End-to-end Form is similar to the schema of Figure 4 in ref 4. In both models, the crystalline layer contains only crystallized methylene units in the *n*-alkyl chains, and the amorphous layer contains the main chains and a portion of the *n*-alkyl chain near the main chain because it is not plausible that all the methylene groups in the side chain of atactic polymer are incorporated into the crystalline layer. The crystallized *n*-alkyl chains are assumed to be oriented so that their chain axes are perpendicular to the interface between the crystalline and amorphous layers. In the amorphous layer, the averaged direction of the main chain is parallel to the interface because of the covalent bonds between the side chain and main chain. As a result, the main chain may take a prolate conformation in the confined amorphous layer, which is like the main chain of side-chain liquid-crystalline polymers in smectic phase.[16] The difference between these two models is the packing manner of the *n*-alkyl chain in the crystalline layer. In Interdigitating Form, the *n*-alkyl chains which are extending from both sides of the crystalline layer are

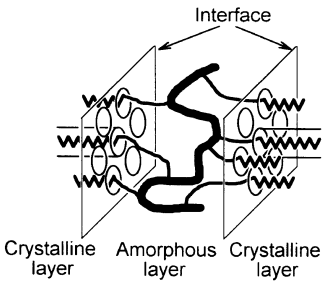

Figure 6. Schematic illustration of chain packing of the side-chain crystallizable comb-like polymer in alternating crystalline-amorphous layered structure. Thick and thin lines represent main chain and side chains, respectively. Cylinders indicate the hexagonally-packed *n*-alkyl chains.

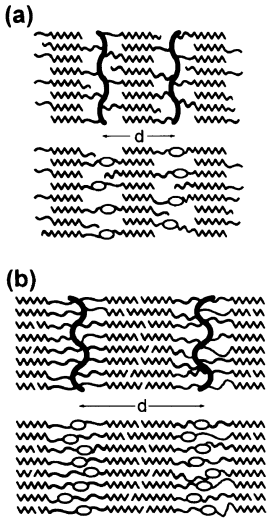

Figure 7. Models for the crystalline-amorphous layered structure. (a) Interdigitating Form and (b) End-to-end Form. The upper and lower figures in both models are illustrated in the same way as the middle and bottom figures in Figure 1.

interdigitated with each other, and the terminal methyl groups in the side chains are located around the interface. In End-to-end Form, the *n*-alkyl chains are packed in an end-to-end manner, and the terminal methyl groups should be located in the middle of the crystalline layer. The area of the interface can be determined by the number of the hexagonally-crystallized *n*-alkyl chain, and so, varies with the change of the packing manner. From the wide-angle X-ray diffraction peak at $2\theta=21°$, which gives the interchain distance for the crystallized *n*-alkyl chain in the hexagonal lattice, the area, A_{side}, of cross-section perpendicular to the chain axis of one crystallized *n*-alkyl chain is obtained to be 20.4 Å^2. If m methylene units in one *n*-alkyl chain are included in the crystalline layer, the width of the crystalline layer in Figure 7 will be expressed by $m \cdot P_{CH_2}$ for Interdigitating Form and $2m \cdot P_{CH_2}$ for End-to-end Form, where P_{CH_2} is the pitch for one CH_2 unit along the chain axis of the crystallized *n*-alkyl chain. Assuming that the volume of the amorphous layer per $-CH_2-CH-$ unit of the main chain, v_{amorph}, is the sum of the volume of amorphous poly(methyl acrylate) (v_{PAO}) and volume of CH_2 groups (v_{CH_2}) in amorphous state, v_{amorph} can be expressed, with considering the composition of *n*-alkyl chain, by

$$v_{amorph} = v_{PA0} + v_{CH_2}(m_t - m)(1/f_{main}) \quad (1)$$

In eq 1, m_t is the number of the methylene unit in one *n*-alkyl chain and $m_t = 17$ is used in the present case. The term $(m_t - m)$ means the averaged number of the methylene unit in the amorphous layer per *n*-alkyl chain. The volume of the amorphous layer corresponding to one *n*-alkyl chain is $v_{amorph} \cdot f_{main}$ for Interdigitating Form and $2v_{amorph} \cdot f_{main}$ for End-to-end Form, and the width of the amorphous layer can be obtained by dividing these values by A_{side}. Finally, the layer spacing d_{calc} is calculated by the sum of the widths of the crystalline and amorphous layers.

$$d_{calc} = (v_{amorph} \cdot f_{main})/A_{side} + m \cdot P_{CH_2} \quad \text{for Interdigitating Form} \quad (2)$$

$$d_{calc} = (2v_{amorph} \cdot f_{main})/A_{side} + 2m \cdot P_{CH_2} \quad \text{for End-to-end Form} \quad (3)$$

The following values are used for calculations[17]: $v_{PA0} = 116.8\,Å^3$, $v_{CH_2} = 27.3\,Å^3$, and $P_{CH_2} = 1.25\,Å$. From the experimentally-obtained heat of fusion, Jordan *et al.*[4] deduced that *ca.* 9 methylene units are crystallizing in one side chain for solid-state poly(*n*-octadecyl acrylate), and $m = 10$ will be used in the following calculations. In practice, change of the value of m has little effect on the calculated layer spacing, so we can obtain d_{calc} as a function of $1/f_{main}$ for both packing models.

The results are drawn by the solid curves in Figure 5. The value of d_{calc} decreases in inversely-proportional manner with the increase of $1/f_{main}$. This phenomenon can be interpreted by the schematic illustration in Figure 8. When the relative number of the *n*-alkyl chain to the repeating unit of main chain is small, the main chain can take a relatively flexible conformation something like Figure 8a. With the increase of $1/f_{main}$, possible conformations for the main chain may be restricted, and the main chain should be confined in the narrow amorphous layer (Figure 8b). These figures suggest that the comb-like polymer having a lot of side chains can not be packed into Interdigitating Form because of the excess number of the crystalline *n*-alkyl chain as compared with the volume of the amorphous layer. If the largest size of the area at the interface for one repeating unit of main chain of poly(methyl acrylate) can be evaluated, we may calculate an upper limit of $1/f_{main}$ to take the packing manner of Interdigitating Form. Now, we tentatively consider interchain distance of the amorphous poly(methyl acrylate) as follows. Contour length of one repeating unit of locally-extended main chain is 2.5 Å. When the side chain methyl ester group is fully-extended, the terminal hydrogen atom in the methyl group locates for 4.46 Å apart from the main chain. From these dimensions and the molecular volume of one monomer unit ($v_{PA0} = 116.8\,Å^3$), the interchain distance is calculated to be 5.2 Å. Therefore, the area at the interface for one monomer unit is obtained as $13.1\,Å^2$, which corresponds to the upper limit for the comb-like polymer in order to pack into Interdigitating Form. Comparison of this value with the cross-section A_{side} of one hexagonally-packed *n*-alkyl chain ($20.4\,Å^2$) suggests that the comb-like PA*x* can not be packed into Interdigitating Form when the side-chain composition is greater than 0.64 ($= 13.1/20.4$) because the side chains are attached too crowdedly to the main chain. Similar calculation has been also conducted for End-to-end Form, and the upper limit of the side-chain composition is evaluated to be 1.28. Then, the curves for d_{calc} in Figure 5 terminate at $1/f_{main} = 0.64$ for Interdigitating Form and at 1.28 for End-to-end Form.

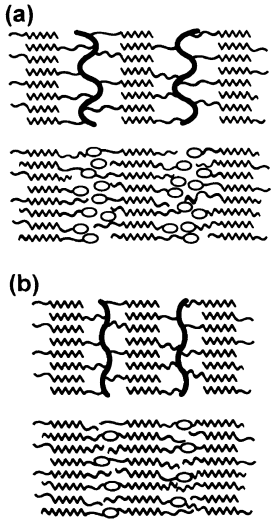

Figure 8. Packing manner of the comb-like chains in Interdigitating Form when the composition of the side chain is large (a) and small (b). See legend to Figure 7.

The experimentally-obtained layer spacings for PA33, PA54, and PA70, and their blends with C18 ($1/f_{main} = 0.33$—0.71), are well reproduced by Interdigitating Form as seen in Figure 5. Around the region of $1/f_{main} = 0.73$—0.89, the X-ray profiles suggest the coexistence of two kinds of the layered structure for both pure and blend samples. The value of $1/f_{main} = 0.73$ is similar to the upper limit of $1/f_{main} = 0.64$ for Interdigitating Form calculated above. The sharp and intense reflections are observed in the profiles of PA100/C18 system, and the layer spacings of which are *ca.* 53 Å. This value is found to be well explained by End-to-end Form as shown by the filled squares at $1/f_{main} = 1.06$, 1.12, and 1.28 in Figure 5, which correspond to the profiles of 6, 11, and 22 mol% C18 content in Figure 3, respectively. In the blends with $1/f_{main} > 1.28$, crystallization of the isolated C18 molecules occurs as shown in the profile of PA100/C18 with 33 mol% C18 in Figure 3. The value of $1/f_{main} = 1.28$ is comparable with the upper limit in order to pack the chain into End-to-end Form as described above.

From these observations, we infer the following mechanism of the transformation of the layered structure of PA*x* and its blends with C18. When there are not so many crystallizable *n*-octadecyl side chains or C18 molecules as compared with the repeating unit of the main chain, the *n*-alkyl chains extending from opposite side of the crystalline layer interdigitate with each other in order to closely pack. With the increase of the number of the *n*-alkyl chain, Interdigitating Form constrains the main chain to take an extended conformation. When the value of $1/f_{main}$ exceeds the limit described above, the polymer and C18 can not be packed into Interdigitating Form and transform to End-to-end Form. Both structural models in Figure 7 are assumed an ordered packing, *i.e.*, the chain axes of the crystallized *n*-alkyl

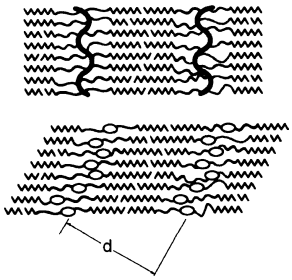

Figure 9. Schematic representation of disordered End-to-end Form. See legend to Figure 7.

chains are perpendicular to the interface between the crystalline and amorphous layers. The sharpness of reflections at $d \approx 30$ Å and 50 Å, which are respectively estimated to originate from Interdigitating and End-to-end Form, suggests the highly-ordered layered structure. Here we consider the relatively broad reflection of $d \approx 40$ Å, which seems to coexist with the sharp reflection as seen in Figures 2 and 3. The transformation from Interdigitating Form to End-to-end Form will result in a decrease of the area of the interface and a sudden change of the balance of the volume of the crystalline and amorphous layers, and will make it difficult to take a regularly arranged structure in Figure 7. One way to cancel this imbalance of the volume of these two layers is to pack the chains with the interface inclined as illustrated in Figure 9, which enlarges the area of the interface. The packing manner in Figure 9, which we will call disordered End-to-end Form, reduces the layer spacing than that of End-to-end Form in the regularly arranged packing. So as not to disturb the hexagonally-packed crystalline order, it seems most plausible that the chains pack in a way such that the position of the interface is shifted by one crystallographical repeating unit, *i.e.*, two methylene units, from that of the neighboring *n*-alkyl chain (Figure 9). By use of the repeating distance along the chain axis of the crystallized *n*-alkyl chain ($2P_{CH_2}$) and the interchain distance for the hexagonal lattice (4.85 Å), the layer spacing d for PA100 ($l/f_{main} = 1.0$) in this packing manner is calculated to be 42.5 Å, which well reproduces the experimental value. From these considerations, it follows that the layered structure of PA100 can be described by disordered End-to-end Form, which is the transient structure between the regularly ordered packing manner, *i.e.*, Interdigitating and End-to-end Form. Disordered End-to-end Form coexists with Interdigitating Form in the range of $1/f_{main} = 0.73$—0.89 as shown in Figure 5. The orderliness of the interface of disordered End-to-end Form may be worse than that of the ordered arrangements, which is the probable reason that the reflection peak in the X-ray profile of PA100 is broad. The transformation of the layered structure observed in PA100/C18 system can be said to be induced by the incorporation of C18 molecules into the crystalline lattice of the side chain[15] as shown in Figure 10.

DSC Measurements for PA100/C18 System

In DSC cooling thermograms of PA100/C18 blends measured at the rate of 20 deg min^{-1}, split of the transition peak for the cocrystallization of C18 with side chain has been observed as commented in Part I of this series.[15] For the blends containing other copolymers, such thermograms have not been obtained. DSC thermograms of PA100/C18 are measured at slower cooling rate (5 deg min^{-1}) and shown in Figure 11. Shapes and temperatures of the transition peaks vary with the change of C18 content in a complicated manner. Crystallization temperature of the blend with 6 mol% C18 is slightly lower than that of pure PA100, and for the blends of 11 mol% and 22 mol%, crystallization temperatures increase with the increase of C18 content. A subsequent peak appears in the thermogram of 22 mol%, and the height of this peak becomes large with the increase of C18 content (22—43 mol%). At a higher temperature, a broad peak can be seen in the thermogram of 43 mol%. Its height and temperature increase with C18 content (43—91 mol%), and the temperature approaches the crystallization point of pure C18. On the other hand, height of the peak at lower temperature is

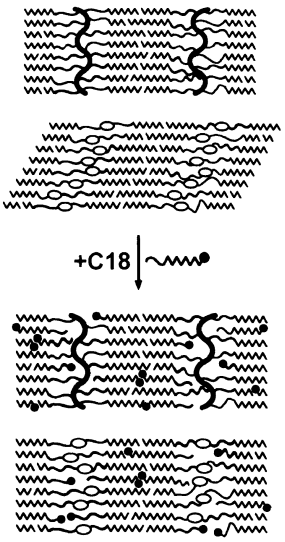

Figure 10. Transformation of the layered structure of PA100 induced by the addition of C18 molecules, which are represented by notched thin line with filled circle. See legend to Figure 7.

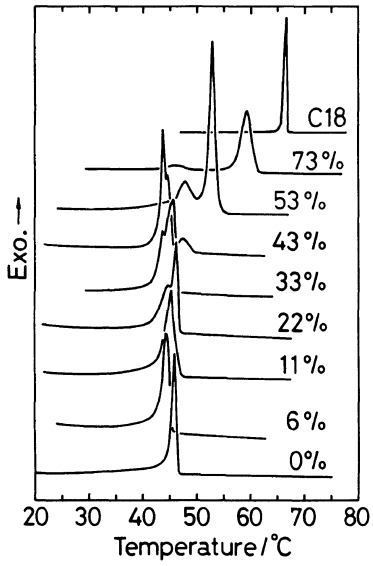

Figure 11. DSC cooling thermograms for PA100/C18 blends with the shown C18 content (mol%), measured at the rate of 5 deg min^{-1}.

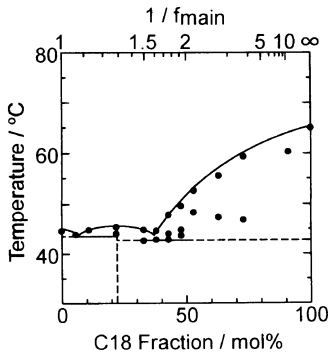

Figure 12. Plots of the crystallization temperature of PA100/C18 blends obtained from the DSC cooling thermogram in Figure 11 against the fraction of C18. Expected liquidus curves and eutectic lines are also shown. In the upper axis, values of $1/f_{main}$, which are equivalent to the mole fraction of C18 in the lower axis, are graduated.

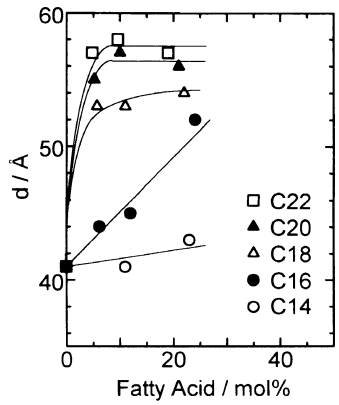

Figure 13. Layer spacings d of blends of PA100 with C14, C16, C18, C20, and C22 as a function of the mole fraction of added fatty acid.

decreased with the increase of C18 content. These complicated behaviors in DSC thermogram of PA100/C18 have not been observed in thermograms measured at the faster cooling rate of 20 deg min^{-1}, or the heating rate of 5 deg min^{-1} for the samples cooled at 5 deg min^{-1} in advance. The crystallization temperatures obtained from Figure 11 are plotted against mole fraction of C18 in Figure 12. This diagram may be interpreted with assuming the formation of a new crystalline form at the fraction of *ca.* 22 mol%, *i.e.*, an eutectic crystallization of the new crystalline form with the crystallite of PA100 occurs in the range of 0—22 mol%, and another eutectic crystallization of the new form with the crystallite of C18 occurs in the range of 22—100 mol%. Expected liquidus curves and eutectic lines are also drawn by solid lines in Figure 12.

In the upper axis of Figure 12, values of $1/f_{main}$, which is equivalent to the mole fraction of C18 in the lower axis, are graduated. The blends of PA100/C18 correspond to the region of $1/f_{main} > 1.0$, where the distinct change in X-ray profiles has been observed as seen in Figure 3 and Figure 5. The new crystalline form at 22 mol% C18 content recalls End-to-end Form described in the preceding section. The above interpretation for the phase behavior can describe the change of the X-ray profiles in Figure 3. Although the coexistence of the ordered and disordered arrangements of End-to-end From is not clearly confirmed because the peak for the latter form is diffuse (see the profiles of 6 and 11 mol% C18 content), the profile for 33 mol% C18 suggests the coexistence of End-to-end Form and C-form of C18.[15,18] The fraction of 22 mol% C18 corresponds to $1/f_{main} = 1.28$, which is comparable with the upper limit in order to pack into End-to-end Form (see the preceding section). These results of DSC measurements confirm the transformation of the layered structure described above.

The diagram in Figure 12 is similar to the phase diagram of the system of poly(ethylene oxide) (PEO) with resorcinol,[19] which is known to form 2:1 stoichiometry molecular complex. In its phase diagram, there exist two eutectic points, *i.e.*, pure PEO with the molecular complex, and pure resorcinol with the molecular complex. Flexible PEO chain is also reported to form complex with urea, $HgCl_2$, $CaCl_2$, and so on, by the force of hydrogen bond.[20] In PA100/C18 system, a possible interaction between the side chain of PA100 and C18 is van der Waals interaction, which is weaker than the interaction of hydrogen bond. However, because of the strong necessity to avoid the imbalance between the volume of crystalline and amorphous layers by the cocrystallization, the PA100/C18 blends are considered to show the phase behavior similar to that of the strongly-interacted PEO/resorcinol system.

Dependence of Chain Length of Fatty Acid

In the above sections in Discussion, we have discussed the structure and phase behavior of PAx/C18 systems. In this section, the dependence of chain length of the added n-alkyl fatty acid on the X-ray profile will be considered. The observed layer spacings d of the blends of PA100 with C14, C16, C18, C20, or C22 are plotted against the fraction of fatty acid in Figure 13. In this figure, we show only data of the samples in which no crystallization of the isolated Cn has been confirmed. In the case of C18, C20, and C22, the addition of small amount of fatty acid induces a distinct increase of d. The value of d increases with the chain length of the added fatty acid. In the case of PA100/C16, the layer spacing increases slowly with C16 content. However, in the system containing short C14 chain, such distinct change in profile can not be recognized as shown in Figure 4.

The transformation of the layered structure for PA100/C18 is considered to be induced by the increase of the volume of the crystalline domain by the cocrystallization of C18 with the side chain of PA100 (Figure 10). The sudden increase of the layer spacing observed in the systems PA100/C20 and PA100/C22 suggests the occurrence of the structural transformation similar to that of PA100/C18. As described in the second section of Discussion, we assume that m methylene groups are crystallizing in one n-alkyl chain and the other $(17-m)$ methylenes are in the amorphous layer for PA100/C18 system. If the value of m shows a little change even when C20 or C22 is added, which seems plausible when the fraction of fatty acid is small, there may be more methylene groups in the amorphous layer than the case of PA100/C18 system. Increase of the volume of the amorphous layer means the decrease of $1/f_{main}$, which increases the layer spacing as shown in Figure 5. This consideration can interpret the finding that the layer spacing is increased with the increase of

chain length of the added *n*-alkyl fatty acid.

On the other hand, in the system of C16 and C14, the sudden increase of layer spacing is not observed as shown in Figure 13. This means that, in order to transform the layered structure as shown in Figure 10, the added fatty acid is needed to have a longer chain length than the side chain of the comb-like polymer. When the chain length of added Cn is short, the fatty acid can not cocrystallize with the side chain and may exist mainly in the amorphous layer. This suggests that, in the blend of comb-like polymer with Cn, the location of the fatty acid in the layered structure depends on its chain length. There have been some reports on molecular-weight dependence of spatial distribution of added homopolymer in the microphase-separated domain of diblock copolymers.[21-23]

CONCLUDING REMARKS

The crystalline-amorphous layered structure of side-chain-crystallizable comb-like polymers, PA*x*, and their blends with *n*-alkyl fatty acid, Cn, has been investigated by X-ray diffraction measurements conducted at room temperature. In PA*x*/C18 systems, the X-ray diffraction profiles in small-angle region vary with the composition of *n*-octadecyl side chain of PA*x* or C18 content in the blends. The tendency of the variation of d for PA*x*/C18 blends with $1/f_{main}$ is similar to that for pure PA*x*, which suggests that the added C18 molecules are cocrystallizing with the side chain and behave like the *n*-alkyl side chain. The observed d values are well interpreted by the transformation of layered structure in the order of Interdigitating Form, disordered End-to-end Form, and End-to-end Form with the increase of $1/f_{main}$. The plots of the crystallization temperature of PA100/C18 obtained from the peak in DSC cooling thermograms suggest the existence of a new crystalline form, which is consistent with the results of the X-ray diffraction measurements. The structural transformation is also recognized in the systems of PA100/C20 and PA100/C22, however, the blends containing *n*-alkyl fatty acid shorter than C18 do not show such distinct change in the X-ray profile.

In this paper, we have shown the possibility to control the transformation of the layered structure and its domain spacing of the comb-like polymers by changing the balance of the volume of the crystalline and amorphous layers, *i.e.*, changing the composition of the long *n*-alkyl side chain by copolymerization and/or addition of *n*-alkyl fatty acid with various chain length.

We have also tried to plot the value of d for the systems of polymethacrylates, PM*x*. From the structural consideration, all the series of PM*x* prepared in Part I[15] (PM16, PM43, PM53, PM71, and PM100) should pack into Interdigitating Form. However, the experimentally-obtained layer spacing shows a weaker dependence on the change of $1/f_{main}$ than the theoretically-expected one. As discussed in Part I,[15] the crystallization behavior of the side chain of PM*x* is influenced by the structure of main chain more strongly than that of PA*x*, which is the result of the difference in the segmental mobility of main-chain group. Namely, in PA*x* series, the high segmental mobility of the main chain do not prevent the side chain from the regular packing. By the same reason, the assumption in the proposed layered structures that there are few defects in the crystalline layer may be attained not in the systems of PM*x*, but in those of PA*x* only. This is the reason why the PA*x*/C18 systems show the drastic change in the layered structure with the change of the fraction of *n*-alkyl chain.

REFERENCES

1. N. A. Platé and V. P. Shibaev, *J. Polym. Sci., Macromol. Rev.*, **8**, 117 (1974).
2. N. A. Platé, V. P. Shibaev, B. S. Petrukhin, Yu. A. Zubov, and V. A. Kargin, *J. Polym. Sci., A-1*, **9**, 2291 (1971).
3. H. W. S. Hsieh, B. Post, and H. Morawetz, *J. Polym. Sci., Polym. Phys. Ed.*, **14**, 1241 (1976).
4. E. F. Jordan, Jr., D. W. Feldeisen, and A. N. Wrigley, *J. Polym. Sci., A-1*, **9**, 1835 (1971).
5. J. M. Barrales-Rienda, F. Fernandez-Martin, C. R. Galicia, and M. S. Chaves, *Makromol. Chem.*, **184**, 2643 (1983).
6. K. Yokota, T. Kougo, and T. Hirabayashi, *Polym. J.*, **15**, 891 (1983).
7. J. Watanabe, H. Ono, I. Uematsu, and A. Abe, *Macromolecules*, **18**, 2141 (1985).
8. M. Ballauff, *Angew. Chem. Int. Ed. Engl.*, **28**, 253 (1989).
9. B. R. M. Gallot, *Adv. Polym. Sci.*, **29**, 85 (1978).
10. T. Inoue, T. Soen, T. Hashimoto, and H. Kawai, *J. Polym. Sci., A-2*, **7**, 1283 (1969).
11. T. Ono, H. Minamiguchi, T. Soen, and H. Kawai, *Kolloid Z.-Z. Polym.*, **250**, 394 (1972).
12. T. Hashimoto, H. Tanaka, and H. Hasegawa, in "Molecular Conformation and Dynamics of Macromolecules in Condenced Systems," M. Nagasawa Ed., Elsevier Science Publishers B. V., Amsterdam, 1988, p 257.
13. L. Leibler, *Macromolecules*, **13**, 1602 (1980).
14. E. Helfand and Z. R. Wasserman, *Macromolecules*, **9**, 879 (1976).
15. K. Inomata, S. Sakamaki, T. Nose, and S. Sasaki, *Polym. J.*, **28**, 986 (1996).
16. L. Noirez, P. Keller, and J. P. Cotton, *Liq. Cryst.*, **18**, 129 (1995).
17. J. Brandrup and E. H. Immergut Eds., "Polymer Handbook," 3rd ed, John Wiley & Sons, New York, N.Y., 1989.
18. V. Malta, G. Celotti, R. Zannetti, and A. F. Martelli, *J. Chem. Soc. (B)*, 548 (1971).
19. E. Delaite, J-J. Point, P. Damman, and M. Dosière, *Macromolecules*, **25**, 4768 (1992).
20. M. M. Iovleva and S. P. Papkov, *Polym. Sci. U.S.S.R.*, **24**, 236 (1982).
21. T. Nose, *Ann. Rep. NMR Spectrosc.*, **27**, 217 (1993).
22. J. Baba, T. Kubo, A. Takano, and T. Nose, *Polymer*, **35**, 145 (1994).
23. T. Hashimoto, H. Tanaka, and H. Hasegawa, *Macromolecules*, **23**, 4378 (1990).